

# EMISSION LINES FROM NITROGEN-LIKE IONS AND THEIR DIAGNOSTIC USE

P. K. RAJU

*Indian Institute of Astrophysics, Bangalore, India*

and

B. N. DWIVEDI

*Department of Applied Physics, Institute of Technology, Banaras Hindu University, Varanasi, India*

(Received 29 January, 1990)

**Abstract.** Line emissions from nitrogen-like ions Ne IV, Mg VI, and Al VII have been studied as a diagnostic probe for the emitting regions of astrophysical plasma. Line intensities from these ions have been calculated and compared, in this study, with available observational data for solar plasma.

## 1. Introduction

The density diagnostics of solar EUV emission lines from nitrogen-like ions have been studied in the past by Raju (1978), Feldman *et al.* (1978), Bhatia and Mason (1980), and Dwivedi and Raju (1988). In the paper by Raju (1978) only the results were briefly reported. Dwivedi and Raju (1988) reported results, for want of space, on detailed investigations for Si VIII and S X only. The aim of the present paper is to report the investigations on the other relevant ions, namely, Ne IV, Mg VI, and Al VII of the nitrogen sequence. Line intensities from these ions have been computed using a model atmosphere by Elzner (1976).

## 2. Energy Level Diagram for Nitrogen Sequence

The schematic energy level diagram comprising the first thirteen levels is shown in Figure 1. The ground configuration  $2s^2 2p^3$  consists of five fine structure levels  $^4S_{3/2}^0$ ,  $^2D_{5/2}^0$ ,  $^2D_{3/2}^0$ ,  $^2P_{1/2}^0$ , and  $^2P_{3/2}^0$ . The higher configuration  $2s 2p^4$  consists of  $^4P$ ,  $^2D$ ,  $^2S$ , and  $^2P$  states. We have adopted the ordering of various levels as given by Wiese *et al.* (1966, 1969). The level  $^2D_{5/2}^0$  is lower than  $^2D_{3/2}^0$  in our case. This is so up to Mg VI. For Al VII the order is reversed. Bhatia and Mason (1980) obtain level  $^2D_{3/2}^0$  lower than  $^2D_{5/2}^0$ . In addition, the level  $2s 2p^4 \ ^2D_{3/2}$  is higher than the level  $2s 2p^4 \ ^2D_{5/2}$  in our case. Whereas Bhatia and Mason (1980) get these levels reversed.

## 3. Emission Rates

The line emissivity  $E(j, i)$  for a line can be expressed as

$$E(j, i) = \frac{N(j)A(j, i)h\nu(j, i)}{4\pi} \text{ (ergs cm}^{-3} \text{ s}^{-1} \text{ sr}^{-1}\text{)}, \quad (1)$$

*Astrophysics and Space Science* 173: 13–26, 1990.

© 1990 Kluwer Academic Publishers. Printed in Belgium.

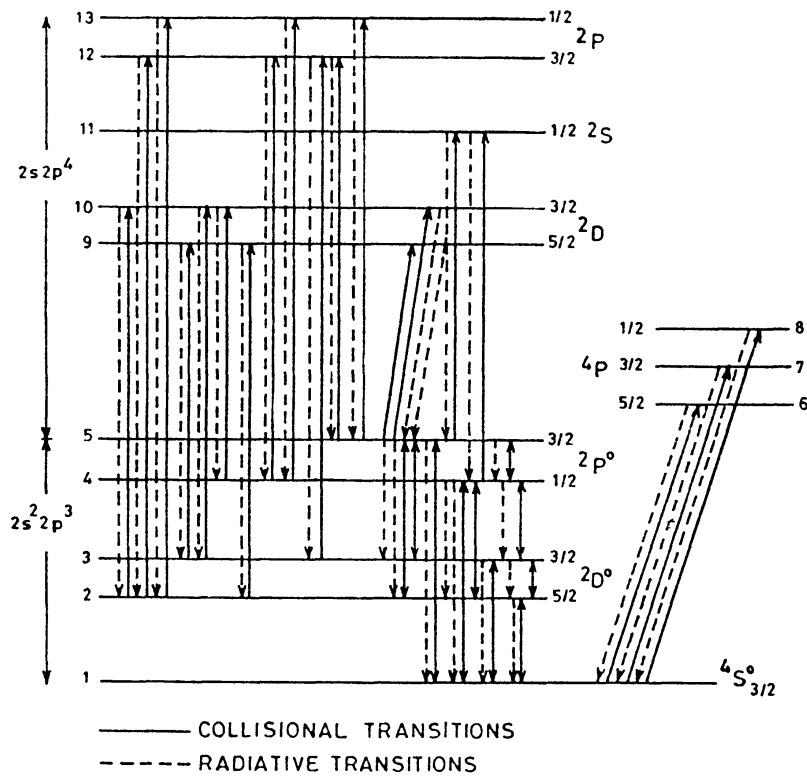


Fig. 1. Energy level diagram for Ni-like ions.

where  $N(j)$  is the level population of the upper level,  $A(j, i)$  is the spontaneous transition probability.  $h\nu(j, i)$  is the energy difference between the lower level  $i$  and the upper level  $j$ . Thus, the problem reduces to the calculation of the level population  $N(j)$ . To compute  $N(j)$  we assume steady-state condition and set up the balance equation for the thirteen levels. The balance equation for the level  $j$  can be written as

$$\begin{aligned}
 N(j) \left[ \sum_{i < j} (A(j, i) + n_e C(j, i)) + \sum_{k > j} n_e C(j, k) \right] = \\
 = \sum_{i < j} N(i) [R(i, j) + n_e C(i, j)] + \sum_{k > j} N(k) [A(k, j) + n_e C(k, j)], \quad (2)
 \end{aligned}$$

where  $n_e$  is the electron density,  $C(m, n)$  are the electron collision rates, and  $R(i, j)$  is the photon-excitation rate. The various physical processes which maintain the steady state for a given level are the following: (i) electron collisional excitations and spontaneous radiative de-excitations for allowed transitions, (ii) electron excitations, electron de-excitations, and spontaneous radiative de-excitations among the ground-term levels. We have neglected the radiative excitations as they are small for electron densities above  $10^7 \text{ cm}^{-3}$ . In Figure 1 the collisional processes are shown by continuous lines and the radiative processes by broken lines.

The collisional rates for forbidden transitions among the ground-term levels are

expressed in terms of collision strengths  $\Omega(i, j)$  as

$$C(i, j) = 8.63 \times 10^{-6} \Omega(i, j) \exp \left[ -\frac{h\nu(j, i)}{kT_e} \right] / \omega(i) T_e^{1/2} \text{ (cm}^3 \text{ s}^{-1}) \quad (3)$$

for excitations ,

$$C(j, i) = C(i, j) \frac{\omega(i)}{\omega(j)} \exp \left[ +\frac{h\nu(j, i)}{kT_e} \right] \text{ (cm}^3 \text{ s}^{-1}) \quad (4)$$

for de-excitations .

In case of allowed transitions the collisional excitation rates are given by the expression

$$C(i, j) = 1.70 \times 10^{-3} gf(i, j) \exp \left[ -\frac{h\nu(j, i)}{kT_e} \right] / T_e^{1/2} W_{ev}(j, i) \text{ (cm}^3 \text{ s}^{-1}), \quad (5)$$

where  $T_e$  is the electron temperature,  $\omega$ 's are the statistical weights,  $f(i, j)$  is the oscillator strength,  $g$  is the Gaunt factor. To facilitate computations we have assumed  $g = 0.5$  for all the transitions.  $W_{ev}(j, i)$  is the energy separation in electron volts.

The emissivity given by Equation (1) can be rewritten as

$$E(j, i) = \frac{1.59 \times 10^{-8}}{4\pi} \frac{A(j, i)}{\lambda(j, i)} \frac{N(j)}{N(\text{ion})} \frac{N(\text{ion})}{N(E)} A(E) n_e \text{ (ergs cm}^{-3} \text{ s}^{-1} \text{ sr}^{-1}), \quad (6)$$

where  $\lambda(j, i)$  is the wavelength in Å.  $N(j)/N(\text{ion})$  is the population of the level  $j$  relative to the total population of the ion  $N(\text{ion})$ .  $N(\text{ion})/N(E)$  is the relative population of the ion, for the element  $E$ .  $A(E)$  is the relative abundance of the element with respect to hydrogen. The relation  $N(\text{H}) = 0.8n_e$  has been used in arriving at Equation (6).  $N(\text{H})$  is hydrogen abundance.  $N(\text{ion})/N(E)$  for the ions Ne IV and Mg VI have been taken from Jordan (1969).  $N(\text{ion})/N(E)$  for Al VII has been taken from Landini and Fossi (1972).

Integrated line intensity at the Sun is given by

$$\begin{aligned} I(j, i) &= \int E(j, i) dh \text{ (cm)} = \\ &= 7.93 \times 10^3 \int n_e E^*(j, i) dh \text{ (km)} \text{ (ergs cm}^{-2} \text{ s}^{-1} \text{ sr}^{-1}). \end{aligned} \quad (7)$$

where

$$E^*(j, i) = 1.59 \times 10^{-8} \frac{A(j, i)}{\lambda(j, i)} \frac{N(j)}{N(\text{ion})} \frac{N(\text{ion})}{N(E)} A(E). \quad (8)$$

Height  $h$  is expressed in km. Line intensities have been computed by using spherically-symmetric model for the quiet Sun (Elzner, 1976).

#### 4. Atomic Data

The atomic data needed to compute  $N(j)$  and, hence, line intensities are the following: (i) wavelengths, (ii) the radiative transition probabilities, and (iii) collision strengths and oscillator strengths.

The wavelengths were taken from Wiese *et al.* (1966, 1969) and Kelly and Palumbo (1973). These values were corrected with the help of the recent work of Edlén (1984).

The transition probabilities for allowed transitions have been taken from Wiese *et al.* (1966, 1969). These values were then plotted against  $(z + 1)$ , where  $z$  is the residual change on the ion. A smooth curve, visually, was drawn for a given transition belonging to various ions in the NI-isoelectronic sequence. In actual computations we have used the values given by Wiese *et al.* (1966, 1969) which do not differ more than 5% from the values lying on the smooth curve. In other cases we have used the values lying on the plotted curve. The same reasoning applies to the various oscillator strengths. In the case of Mg VI ion we have compared the values used by us with those of Bhatia and Mason (1980). The transition probability and oscillator strength for  ${}^2D_{3/2} \rightarrow {}^2P_{3/2}^0$  calculated by Bhatia and Mason (1980) is smaller by a factor of 3. The transition probability and oscillator strength for the transition  ${}^2P_{1/2} \rightarrow {}^2P_{3/2}^0$  used by us is smaller by a factor of 2 as compared to the ones obtained by Bhatia and Mason (1980). The values for the other transition probabilities and oscillator strengths differ by a factor up to 20%.

The radiative probabilities for the forbidden lines have been taken from Wiese *et al.* (1966, 1969). These have been compared with the ones obtained by Bhatia and Mason (1980) and Zeippen (1982). For Ne IV and Mg VI the values used by us are nearly the same as the ones obtained by Zeippen (1982). In the case of Al VII, the values for the transitions  ${}^2D_{5/2}^0 \rightarrow {}^4S_{3/2}^0$  and  ${}^2D_{3/2}^0 \rightarrow {}^4S_{3/2}^0$  used by us are smaller by a factor of 2 to the ones calculated by Zeippen (1982). The values for the other transitions differ up to a maximum of 30% in the case of the transition  ${}^2D_{3/2}^0 - {}^2D_{5/2}^0$ . The values for Mg VI calculated by Zeippen lie intermediate to the ones used by us and Bhatia and Mason. The radiative probabilities obtained by Bhatia and Mason for the transitions  ${}^2P_{1/2}^0 \rightarrow {}^2D_{5/2}^0$  and  ${}^2P_{3/2}^0 \rightarrow {}^2P_{1/2}^0$  for Mg VI are smaller by a factor 2 and 3, respectively, to that of Wiese *et al.* (1969).

The known collision strengths have been taken from Saraph *et al.* (1969) and Czyzak *et al.* (1974). The known collision strengths for a given transition for the various ions in the NI-sequence have been plotted against  $(z + 1)$ .  $z$  is the residual charge on the ion. As before, a smooth curve has been drawn for a given transition. We have used, in addition, for some transitions the infinite limit value for the collision strength given by Saraph *et al.* (1969). The known value of collision strengths used by us differ rather slightly from the ones used by Kafatos and Lynch (1980). Kafatos and Lynch used the threshold values given by Saraph *et al.* While we have used the values corresponding to the next higher energy. The unknown collision strengths have been obtained from the

smooth curve. In case, the known collision strengths differ by more than 10% from the values on the curve we have used the latter values. The collision strengths for Mg VI computed by Bhatia and Mason are smaller than the values used by us. In a few cases they are smaller by 60%. Our value of collision strength for the transition  ${}^2D_{3/2}^0 \rightarrow {}^2D_{5/2}^0$  is greater by a factor of 2 from that of Bhatia and Mason.

### 5. Results and Discussion

The occupation of higher levels is essentially governed by the levels of the ground state. Therefore, the variation in the population of ground term levels is reflected in the variation of line intensities. The relative ion abundance of an element peaks at a particular temperature. Thus, it is reasonable to assume that a line is effectively emitted from a thin layer of constant electron density and temperature. We have shown, in Figures 2 to 4, the relative population of ground levels as a function of electron density for Ne IV, Mg VI, and Al VII. The temperature indicated in these figures correspond to the maximum relative ionic abundance of the element. We find that the ground term level

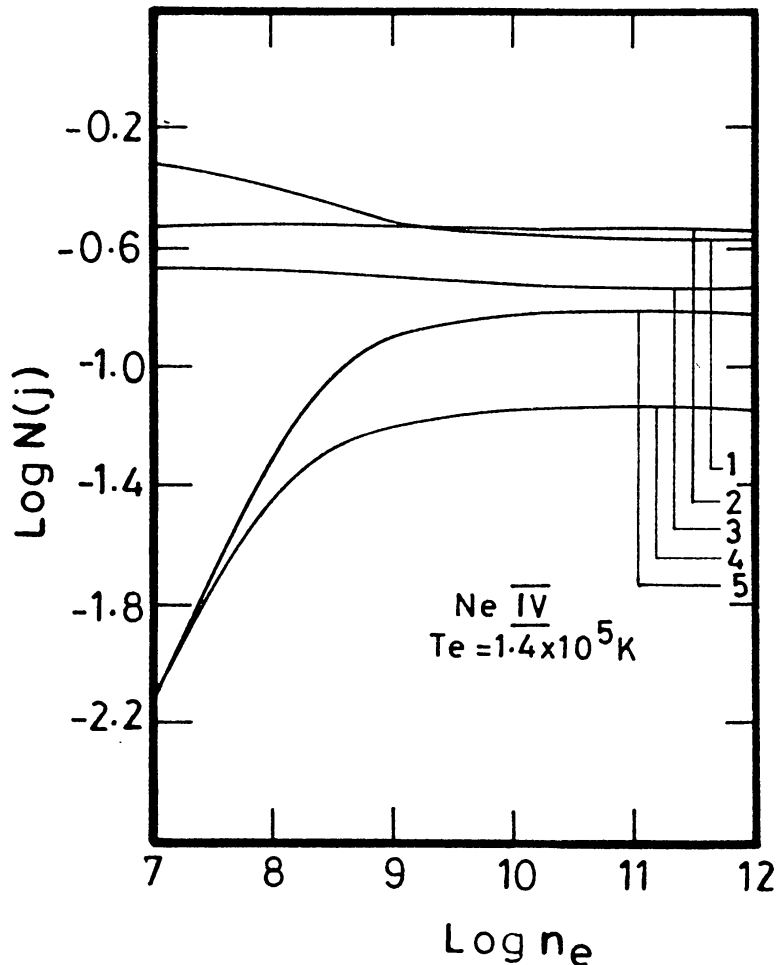


Fig. 2. Relative population of ground term levels  $N(j)$  of Ne IV as a function of electron density  $n_e$ .

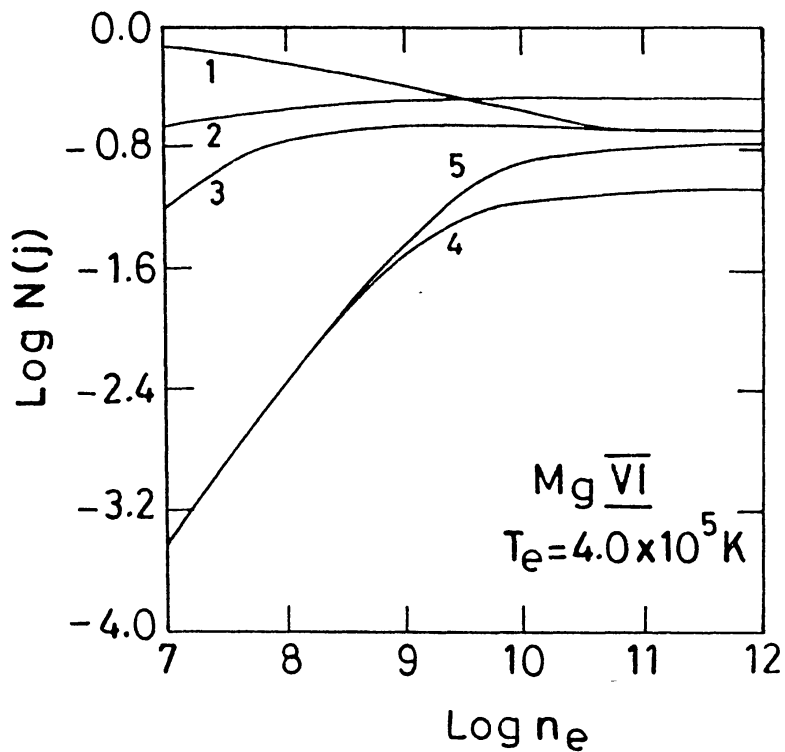


Fig. 3. Same as Figure 2 but for Mg VI.

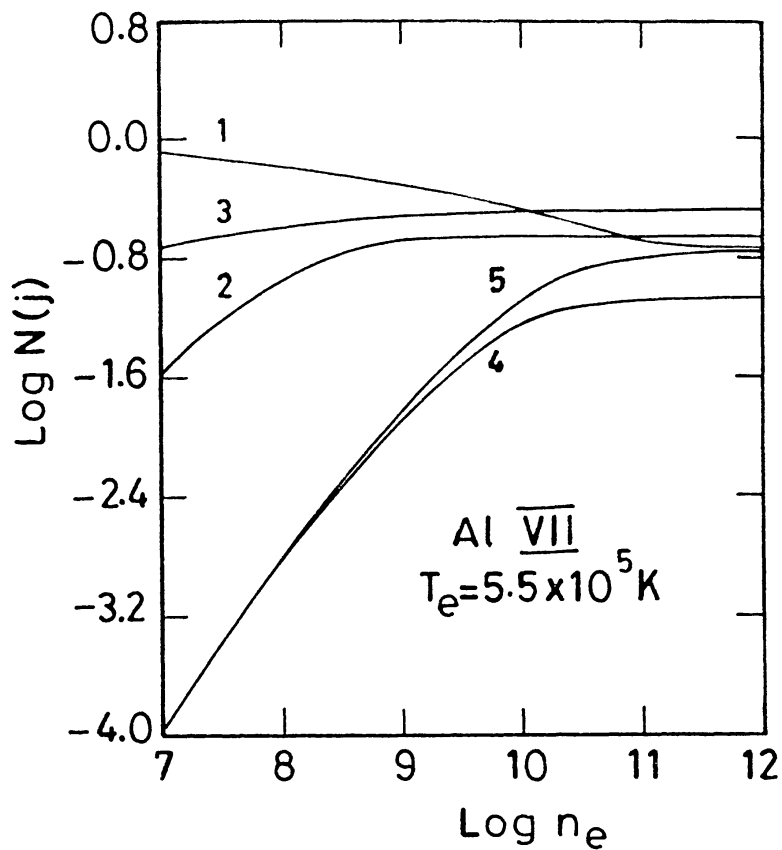


Fig. 4. Same as Figure 2 but for Al VII.

populations vary with electron density. Therefore, the line intensities which are due to excitations from the ground term would be sensitive to electron density variations.

We have given in Table I the relative populations of the ground state levels obtained by us and by Bhatia and Mason for the Mg VI ion. It must be kept in mind, while comparing, that the energy ordering of the levels  ${}^2D_{3/2}^0$ ,  ${}^2D_{5/2}^0$ ,  ${}^2D_{3/2}$ , and  ${}^2D_{5/2}$  obtained by Bhatia and Mason are inverse of the ones used by us. The discrepancies for levels 2 and 3 could be due to the different ordering of energy levels.

In addition, we have not considered the rates from the levels 2, 3, 4, and 5 to the levels 6, 7, and 8, respectively. In case of Mg VI ion the neglect of the sum of rates  $2 \rightarrow 6$ ,  $3 \rightarrow 6$ ,  $4 \rightarrow 6$ , and  $5 \rightarrow 6$  in the rate  $1 \rightarrow 6$  to populate level 6 leads to an error of 5%. It is about 10% for the level 7, and about 15% for the level 8. Furthermore, in the equilibrium equations, the de-population rate for 2, 3, 4, and 5, respectively, is underestimated by

TABLE I  
Relative population of ground term levels  $N(j)/N(\text{ion})$  for Mg VI

Ion	$j$	$N(j)/N(\text{ion})$ for $n_e$ ( $\text{cm}^{-3}$ )				
		$10^8$	$10^9$	$10^{10}$	$10^{11}$	$10^{12}$
Mg VI ${}^4S_{3/2}^0$	1	0.53 <sup>r</sup>	0.42	0.27	0.21	0.21
		0.62	0.50	0.35	0.29	0.29
${}^2D_{5/2}^0$ ${}^2D_{3/2}^0$	2	0.27	0.30	0.32	0.33	0.33
		0.15	0.19	0.20	0.20	0.20
${}^2D_{3/2}^0$ ${}^2D_{5/2}^0$	3	0.18	0.22	0.21	0.21	0.21
		0.22	0.24	0.28	0.29	0.29
${}^2P_{1/2}^0$	4	0.46–2	0.31–1	0.71–1	0.84–1	0.85–1
		0.50–2	0.31–1	0.65–1	0.75–1	0.76–1
${}^2P_{3/2}^0$	5	0.42–2	0.36–1	0.13	0.17	0.17
		0.42–2	0.36–1	0.12	0.15	0.15

<sup>r</sup>: The first row is for our values at  $T_e = 4 \times 10^5$  K. The second row is for the values obtained by Bhatia and Mason (1980) at  $T_e = 5 \times 10^5$  K.

about 5% when the rates from levels  $2s^2p^3({}^2D^0, {}^2P^0)$  to the levels  $2s2p^4({}^4P)$  are neglected. Similar arguments hold for the neglect of the rates from  $2s^22p^3{}^4S_{3/2}^0$  to the levels  $2s2p^4({}^2D, {}^2S, {}^2P)$ . The neglected collision rates are being incorporated in a subsequent investigation. Bhatia and Mason have not considered Ne IV and Al VII, therefore, we cannot compare the results for these ions.

The computed line intensities along with the observed values for Ne IV, Mg VI, and Al VII are given in Tables II, III, and IV, respectively. The theoretical intensity refers to the disk center. The computed line intensities have been obtained using the model atmosphere of Elzner (1976). The theoretical intensities may be useful in resolving difficulties associated with line identification, masking or blending due to lines arising from ions of other isoelectronic sequences. Such a study provides first-hand information

TABLE II  
Theoretical line intensities using a model atmosphere. Ne IV,  $A(\text{Ne}) (= N(\text{Ne})/N(\text{H})) = 3.98 \times 10^{-5}$

Transition	Wavelength (Å)	Theore- tical	Intensity observed <sup>a</sup>			
			DU	VR	DE	BE
$2s2p^4 \rightarrow 2s^22p^3$						
$^2P_{1/2} - ^2D_{3/2}^0$	357.825	0.92				
$^2P_{3/2} - ^2D_{5/2}^0$	358.688	1.70			6 <sup>b</sup>	5 <sup>b</sup>
$^2P_{3/2} - ^2D_{3/2}^0$	358.746	0.18				
$^2P_{1/2} - ^2P_{1/2}^0$	387.132	0.19				
$^2P_{1/2} - ^2P_{3/2}^0$	387.141	0.09				
$^2P_{3/2} - ^2P_{1/2}^0$	388.209	0.09				
$^2P_{3/2} - ^2P_{3/2}^0$	388.218	0.48				
$^2S_{1/2} - ^2P_{1/2}^0$	421.599	0.25			6.57 <sup>b</sup>	4 <sup>b</sup>
$^2S_{1/2} - ^2P_{3/2}^0$	421.610	0.47				
$^2D_{3/2} - ^2D_{5/2}^0$	469.775	0.12				
$^2D_{3/2} - ^2D_{3/2}^0$	469.874	1.09	6.84		5 <sup>b</sup>	
$^2D_{5/3} - ^2D_{5/2}^0$	469.830	1.98				
$^2D_{5/2} - ^2D_{3/2}^0$	469.929	0.13				
$^2D_{3/2} - ^2P_{1/2}^0$	521.738	0.14				
$^2D_{3/2} - ^2P_{3/2}^0$	521.755	0.03				
$^2D_{5/2} - ^2P_{3/2}^0$	521.823	0.28				
$^4P_{1/2} - ^4S_{3/2}^0$	541.126	0.64			4	
$^4P_{3/2} - ^4S_{3/2}^0$	542.070	1.26	9.46	6.44 <sup>b</sup>	4	
$^4P_{5/2} - ^4S_{3/2}^0$	543.886	1.96		9.13 <sup>b</sup>	5	
$2s^22p^3 \rightarrow 2s^22p^3$						
$^2P_{3/2}^0 - ^4S_{3/2}^0$	1601.43	0.05				
$^2P_{1/2}^0 - ^4S_{3/2}^0$	1601.59	0.01				

<sup>a</sup> DU: Dupree *et al.* (1973); VR: Vernazza and Reeves (1978); DE: Dere (1978); BE: Behring *et al.* (1976); SBT: Sandlin *et al.* (1977)

<sup>b</sup> Cf. text.

#### Notes to Tables II, III, and IV

$N(E)/N(\text{H}) (= A(E))$  is the relative abundance of the element  $E$  with respect to hydrogen. The values for  $A(\text{Ne})$  and  $A(\text{Mg})$  are from Kato (1976). The value for  $A(\text{Al})$  has been taken from Dupree (1978).

Col. 1: Line transitions.

Col. 2: Wavelength in Å. The values are from Edlén (1984).

Col. 3: Theoretical intensities (disk center) in  $\text{ergs cm}^{-2} \text{s}^{-1} \text{sr}^{-1}$ , using the spherically-symmetric model of Elzner (1976).

Cols. 4 and 5: Observed intensities in  $\text{ergs cm}^{-2} \text{s}^{-1} \text{sr}^{-1}$ ; (i) for quiet regions of solar atmosphere at solar maximum, Dupree *et al.* (1973); (ii) for quiet regions at solar minimum, Vernazza and Reeves (1978).

Col. 6: Observed intensities for flare regions during solar minimum (ATM SKYLAB data). The values are on a scale 1 to 10, Dere (1978).

Col. 7: Observed intensities for full-sun solar spectrum obtained by rocket-borne spectrograph. The observed values correspond to solar minimum. Intensity values are only estimates, Behring *et al.* (1976).

Col. 8: Off-limb forbidden line intensities observed from Skylab, Sandlin *et al.* (1977) and Sandlin and Tousey (1979).

We discuss below specifically some of the lines for the respective ions.

Ne IV The line at 358.688 Å is very close to the line at 358.67 Å of Fe XI with intensities 6 (DU) and 5 (BE), respectively. The 421.599 Å and 421.610 Å lines are close to the unidentified lines at 421.8 Å and



TABLE III  
Theoretical line intensities using a model atmosphere. Mg VI,  $A(\text{Mg}) (= N(\text{Mg})/N(\text{H})) = 3.16 \times 10^{-5}$

Transition	Wavelength (Å)	Theoretical	Intensity observed <sup>a</sup>				
			DU	VR	DE	BE	SBT
$2s2p^4 \rightarrow 2s^22p^3$							
$^2P_{1/2} - ^2D_{3/2}^0$	268.991	2.73			b		
$^2P_{3/2} - ^2D_{5/2}^0$	270.390	4.58			b		
$^2P_{3/2} - ^2D_{3/2}^0$	270.400	0.51				5 <sup>b</sup>	
$^2P_{1/2} - ^2P_{1/2}^0$	291.363	0.50					
$^2P_{1/2} - ^2P_{3/2}^0$	291.455	0.25					
$^2P_{3/2} - ^2P_{1/2}^0$	293.016	0.23					
$^2P_{3/2} - ^2P_{3/2}^0$	293.110	1.12			3 <sup>b</sup>		
$^2S_{1/2} - ^2P_{1/2}$	314.540	0.25			b	b	
$^2S_{1/2} - ^2P_{3/2}^0$	314.647	0.49					
$^2D_{3/2} - ^2D_{5/2}^0$	349.108	0.36					
$^2D_{3/2} - ^2D_{3/2}^0$	349.124	3.19			7 <sup>b</sup>		
$^2D_{5/3} - ^2D_{5/2}^0$	349.163	5.02					
$^2D_{5/2} - ^2D_{3/2}^0$	349.179	0.36					
$^2D_{3/2} - ^2P_{1/2}^0$	387.768	0.41			6		
$^2D_{3/2} - ^2P_{3/2}^0$	387.932	0.08					
$^2D_{5/2} - ^2P_{3/2}^0$	388.000	0.74			6		
$^4P_{1/2} - ^4S_{3/2}^0$	399.281	2.23		30.06 <sup>b</sup>	6		
$^4P_{3/2} - ^4S_{3/2}^0$	400.662	4.51			6		
$^4P_{5/2} - ^4S_{3/2}^0$	403.307	6.63		25.73 <sup>b</sup>	6 <sup>b</sup>	7 <sup>b</sup>	
Forbidden transitions							
$^2P_{3/2}^0 - ^4S_{3/2}^0$	1190.12	1.03					114 <sup>b</sup>
$^2P_{1/2}^0 - ^4S_{3/2}^0$	1191.67	0.34					22.5 <sup>b</sup>
$^2D_{3/2}^0 - ^4S_{3/2}^0$	1806.00	0.03					1.8 <sup>b</sup>
$^2P_{3/2}^0 - ^2D_{5/2}^0$	3487.30	0.07					
$^2P_{3/2}^0 - ^2D_{3/2}^0$	3488.90	0.11					
$^2P_{1/2}^0 - ^2D_{3/2}^0$	3502.20	0.06					

<sup>a</sup> DU: Dupree *et al.* (1973); VR: Vernazza and Reeves (1978); DE: Dere (1978); BE: Behring *et al.* (1976); SBT: Sandlin *et al.* (1977).

<sup>b</sup> Cf. text.

421.59 Å with intensities 6.57 (VN) and 4 (DE), respectively. Lines at 469.874 Å and 469.830 Å are close to the unidentified line at 469.84 Å with intensity 5 (DE).

The lines 541.126 Å and 542.070 Å have been identified, probably, with Ne IV lines with intensity 6.44 (VN).

The forbidden lines 1601.43 Å and 1601.59 Å are weak and could be seen only off-limb.

Mg VI: The lines at 268.991 Å and 270.390 Å are weak in Dere's list. Theoretically these lines are rather strong.

The 270.400 Å line is close to the unidentified line at 270.407 Å with intensity 5 (BE).

The 293.110 Å line is close to the line 293.15 Å. Dere (1978) identified the line at 293.15 Å with Cr XXI with intensity 3. The 314.54 Å and 314.647 Å lines blend with strong line of Si VIII at 314.356 Å with intensities 7 (DE) and 6 (BE), respectively. Our theoretical intensity for this Si VIII line is 9.8 (Dwivedi and Raju, 1988).

The line at 349.13 Å has been identified by Dere (1978) with Mg VI line (349.124) with intensity 7. It is puzzling to find that a much stronger line at 349.163 Å is not observed.

The 399.20 Å line has been, tentatively, identified with Mg VI (399.281 Å) line by Vernazza and Reeves, it could blend with the Ne VI line at 399.83 Å. The 403.307 Å line blends with the Ne VI line.

TABLE IV

Theoretical line intensities using a model atmosphere. Al VII,  $A(\text{Al}) (= N(\text{Al})/N(\text{H})) = 3.72 \times 10^{-6}$ 

Transition	Wavelength (Å)	Theoretical	Intensity observed <sup>a</sup>				
			DU	VR	DE	BE	ST
$2s2p^4 - 2s^22p^3$							
$^2P_{1/2} - ^2D_{3/2}^0$	239.022	0.33			2 <sup>b</sup>	16 <sup>b</sup>	
$^2P_{3/2} - ^2D_{3/2}^0$	240.732	0.06			3 <sup>b</sup>	20 <sup>b</sup>	
$^2P_{3/2} - ^2D_{5/2}^0$	240.774	0.54					
$^2P_{1/2} - ^2P_{1/2}^0$	259.020	0.06					
$^2P_{1/2} - ^2P_{3/2}^0$	259.196	0.03					
$^2P_{3/2} - ^2P_{1/2}^0$	261.030	0.03			4 <sup>b</sup>	22 <sup>b</sup>	
$^2P_{3/2} - ^2P_{3/2}^0$	261.208	0.14					
$^2D_{3/2} - ^2D_{3/2}^0$	309.016	0.36					
$^2D_{5/2} - ^2D_{3/2}^0$	309.056	0.05					
$^2D_{3/2} - ^2D_{5/2}^0$	309.085	0.04					
$^2D_{5/2} - ^2D_{5/2}^0$	309.125	0.63					
$^2D_{5/2} - ^2P_{3/2}^0$	343.639	0.10					
$^4P_{1/2} - ^4S_{3/2}^0$	352.159	0.36			6 <sup>b</sup>	20 <sup>b</sup>	
$^4P_{3/2} - ^4S_{3/2}^0$	353.777	0.74			8 <sup>b</sup>	9 <sup>b</sup>	
$^4P_{5/2} - ^4S_{3/2}^0$	356.892	1.13					
$2s^22p^3 \rightarrow 2s^22p^3$							
$^2P_{3/2}^0 - ^4S_{3/2}^0$	1054.00	0.16					
$^2P_{1/2}^0 - ^4S_{3/2}^0$	1056.91	0.07					
$^2D_{3/2}^0 - ^4S_{3/2}^0$	1604.78	0.02					b
$^2P_{3/2}^0 - ^2D_{3/2}^0$	3070.10	0.02					

<sup>a</sup> DU: Dupree *et al.* (1973); VR: Vernazza and Reeves (1978); DE: Dere (1978); BE: Behring *et al.* (1976); ST: Sandlin and Tousey (1979).

<sup>b</sup> Cf. text.

Forbidden lines 1190.12 Å, 1191.67 Å, and 1806.00 Å are weak and have been observed only off-limb. The 3487.30 Å, 3488.9 Å, and 3502.2 Å lines: among the observed lines the line at 3487.30 Å is missing. Theoretical line intensities, Table III and Kastner (1983), indicate that the Mg VI line at 3487.30 Å should also be seen. The absence of the line 3487.30 Å is puzzling.

Al VII: Al VII lines below 1000 Å blend with stronger lines of Fe XI, Fe XIII, and Fe XIV.

The 239.022 Å line is close to an unidentified line at 239.03 Å with intensity 2 (DE) and 16 (BE). 240.774 Å and 240.732 Å. These two lines blend with 240.72 Å of Fe XIV with intensity 3 (D) and 240.713 Å of Fe XIII with intensity 20 (BE).

The 261.030 Å line blends with 261.06 Å line of Si X with intensities 4 (DE) and 22 (BE).

The 352.15 Å line blends with 352.10 Å line of Fe XII with intensities 6 (DE) and 20 (BE).

The 353.777 Å line blends with Fe XIV and Ar XVI with intensities 8 (DE) and 9 (BE).

The 1604.78 Å: it is a weak forbidden line and has been observed off-limb by Sandlin and Tousey (1979). It should be possible to observe a much stronger line of Al VII at 1054.00 Å and 1056.91 Å. The computed intensity of 3070.10 Å line is equal to the computed line intensity of the 1604.78 Å line.

to predict lines that have hitherto not been observed for future observations. In addition, such an investigation could also act as a test or constraint on the model atmosphere when compared with observations.

We have shown in Figures 5, 6, and 7 line intensity ratios as a function of electron

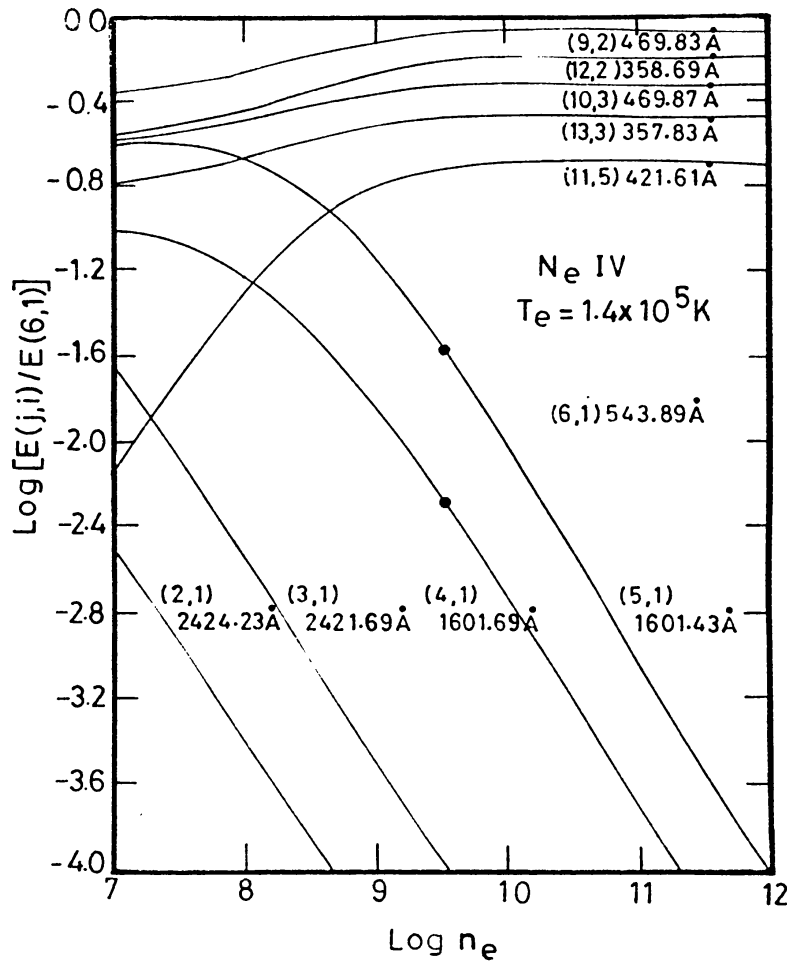


Fig. 5. Log of intensity ratios  $E(j, i)/E(6, 1)$  for Ne IV, at the electron temperature  $T_e$ , as a function of  $\log n_e$ . Filled circles correspond to the theoretical ratios based on the model atmosphere of Elzner (1976).

density for Ne IV, Mg VI, and Al VII, respectively. The temperatures indicated in these figures correspond to the maximum relative ion abundance for the element. Line intensity ratios for Si VIII and S X have already been reported elsewhere (Dwivedi and Raju, 1988). We have indicated by filled circles the theoretical ratios for a model atmosphere. We note from Figure 5 that only the ratios involving forbidden lines fall on the density sensitive portion. These ratios give an average value of  $3.3 \times 10^9 \text{ (cm}^{-3}\text{)}$  for  $n_e$  from Ne IV lines. The other ratios do not lie at any point on the respective theoretical curves. These discrepancies are being looked into.

The average electron density from the theoretical intensity ratios for Mg VI lines is  $1.4 \times 10^9 \text{ (cm}^{-3}\text{)}$  (Figure 6). In Table V we have given theoretical intensity ratios obtained by us and by Bhatia and Mason for some of the lines. We find that our ratios are large by about a factor of 2 for some of the ratios. Figure 7 represents the intensity ratios for Al VII ion. The average electron density from Al VII lines is  $7.6 \times 10^8 \text{ (cm}^{-3}\text{)}$ .

Tables II, III, and IV indicate that the number of observed lines with calibrated intensities are rather few in number for reliable electron density determination.

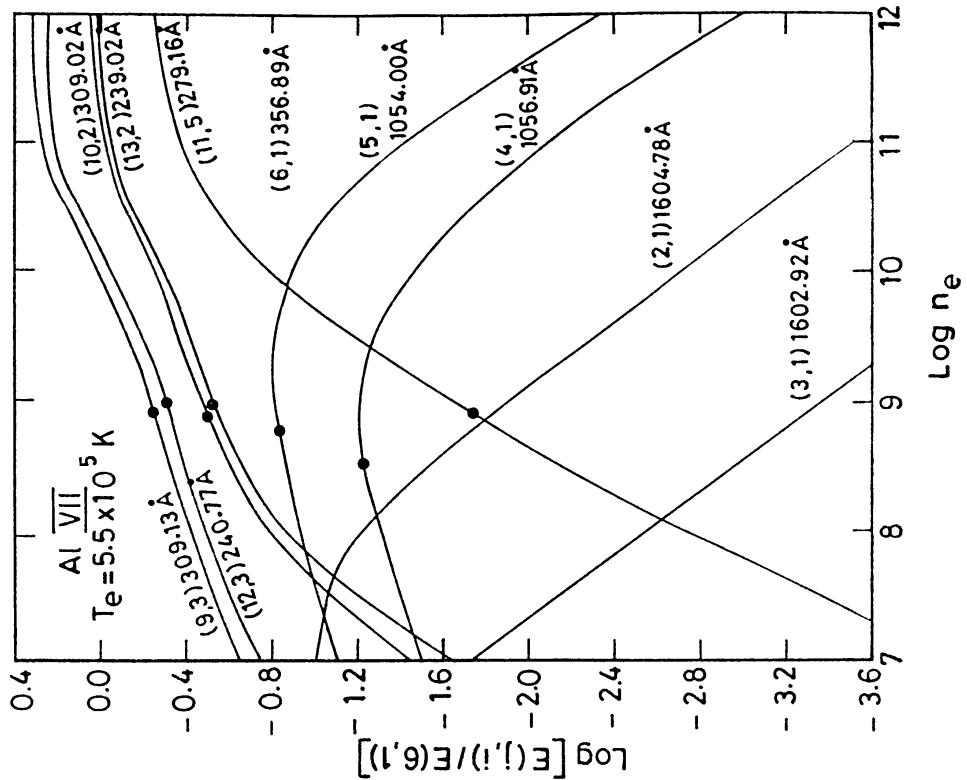


Fig. 7. Same as Figure 5 but for AlVII.

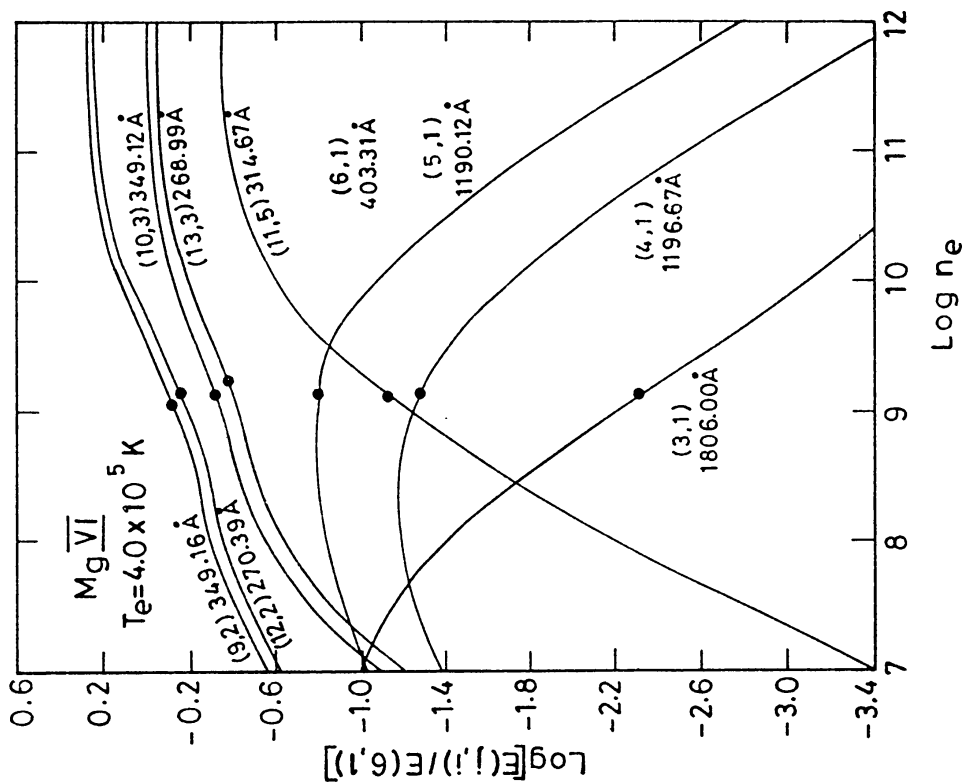


Fig. 6. Same as Figure 5 but for MgVI.

TABLE V

Theoretical intensity ratios, relative to transition  $6 \rightarrow 1$ , for Mg VI lines. First row: our values; second row: values obtained by Bhatia and Mason.

Transition	Wavelength (Å)	Electron density $n_e$				
		$10^8$	$10^9$	$10^{10}$	$10^{11}$	$10^{12}$
$6 \rightarrow 1$	403.307	1.0	1.0	1.0	1.0	1.0
$7 \rightarrow 1$	400.662	0.68	0.68	0.68	0.68	0.68
		0.67	0.67	0.67	0.67	0.67
$8 \rightarrow 1$	399.281	0.33	0.33	0.33	0.33	0.33
		0.35	0.35	0.35	0.35	0.35
$10 \rightarrow 3$	349.124	0.28	0.45	0.73	0.93	0.98
		0.19	0.32	0.50	0.60	0.62
$10 \rightarrow 2$	349.108	0.03	0.05	0.08	0.11	0.11
		0.02	0.03	0.05	0.06	0.06
$9 \rightarrow 2$	349.163	0.48	0.71	1.27	1.70	1.78
		0.26	0.39	0.68	0.85	0.88
$12 \rightarrow 2$	270.390	0.42	0.63	1.18	1.59	1.70
		0.25	0.36	0.64	0.80	0.83
$13 \rightarrow 3$	268.991	0.22	0.37	0.65	0.83	0.87
		0.12	0.20	0.34	0.42	0.43

## 6. Conclusion

In this paper we have seen that emission lines from nitrogen-like ions are useful as a density diagnostic of solar plasma. The theoretical line intensities for Ne IV, Mg VI, and Al VII reported in this paper may be useful in resolving difficulties associated with line identification. The number of observed lines with calibrated intensities are rather few for reliable electron density determination. Therefore, solar spectra in the UV are required with greater spectral resolution and calibrated line intensities.

## Acknowledgement

The authors are grateful to Professor J. C. Bhattacharyya, Director, Indian Institute of Astrophysics, Bangalore for useful suggestions. The authors are grateful to the unknown referee for improving the language of the text.

## References

- Behring, W. E., Cohen, L., Feldman, U., and Doschek, G. A.: 1976, *Astrophys. J.* **203**, 521.  
 Bhatia, A. K. and Mason, H. E.: 1980, *Monthly Notices Roy. Astron. Soc.* **190**, 925.  
 Czyzak, S. J., Aller, L. H., and Euwema, R. N.: 1974, *Astrophys. J. Suppl.* **272**, 465.  
 Dere, K. P.: 1978, *Astrophys. J.* **221**, 1062.  
 Dupree, A. K.: 1972, *Astrophys. J.* **178**, 527.

- Dupree, A. K., Huber, M. C. E., Noyes, R. W., Parkinson, W. H., Reeves, E. M., and Withbroe, G. L.: 1973, *Astrophys. J.* **182**, 321.
- Dwivedi, B. N. and Raju, P. K.: 1988, *Adv. Space Res.* **8**, No. 11, 179.
- Edlén, B.: 1984, *Phys. Scripta* **30**, 135.
- Elzner, L. R.: 1976, *Astron. Astrophys.* **47**, 9.
- Feldman, U., Doschek, G. A., Mariska, J. T., Bhatia, A. K., and Mason, H. E.: 1978, *Astrophys. J.* **226**, 674.
- Jordan, C.: 1969, *Monthly Notices Roy. Astron. Soc.* **142**, 501.
- Kafatos, M. and Lynch, J. P.: 1980, *Astrophys. J. Suppl.* **42**, 611.
- Kato, T.: 1976, *Astrophys. J. Suppl.* **30**, 397.
- Karstner, S. O.: 1983, *Solar Phys.* **85**, 41.
- Kelly, R. L. and Palumbo, L. J.: 1973, *NRL Report* 7599.
- Landini, M. and Monsignori Fossi, B. C.: 1972, *Astron. Astrophys. Suppl.* **7**, 291.
- Raju, P. K.: 1978, *Bull. Astron. Soc. India* **6**, 45.
- Sandlin, G. D., Brueckner, G. E., and Tousey, R.: 1977, *Astrophys. J.* **214**, 898.
- Sandlin, G. D. and Tousey, R.: 1979, *Astrophys. J.* **227**, L107.
- Saraph, H. E., Seaton, M. J., and Shemming, J.: 1968, *Phil. Trans. Roy. Soc. London* **264**, 77.
- Vernazza, J. E. and Reeves, E. M.: 1978, *Astrophys. J. Suppl.* **37**, 485.
- Wiese, W. L., Smith, M. W., and Glennon, B. M.: 1966, *Atomic Transition Probabilities; Hydrogen through Neon*, Vol. 1, Natl. Bur. Standards, Washington.
- Wiese, W. L., Smith, M. W., and Miles, B. M.: 1969, *Atomic Transition Probabilities, Sodium through Calcium*, Vol. 2, Nat. Bur. Standards, Washington.
- Zeippen, C. J.: 1982, *Monthly Notices Roy. Astron. Soc.* **198**, 111.